A 3–5 GHz BPSK transmitter for IR-UWB in 0.18 μm CMOS*

Fu Delong(付德龙), Huang Lu(黄鲁)†, Cai Li(蔡力), and Lin Fujiang(林福江)

(Department of Electronic Science and Technology, University of Science and Technology of China, Hefei 230027, China)

Abstract: This paper presents a transmitter IC with BPSK modulation for an ultra-wide band system. It is based on up-conversion with a high linearity passive mixer. Unlike the traditional BPSK modulation scheme, the local oscillator (LO) is modulated by the baseband data instead of the pulse. The chip is designed and fabricated by standard 0.18 μm CMOS technology. The transmitter achieves a high data rate up to 400 Mbps. The amplitude of the pulse can be adjusted by the amplitude of the LO and the bias current of the driver amplifier. The maximum peak-to-peak amplitude of the pulse is 600 mV. It consumes only 20.3 mA current with a supply voltage of 1.8 V when transmitting a pulse at the maximum data rate. The energy efficiency is 91.4 pJ/pulse. The die area is 1.4×1.4 mm^2.

Key words: transmitter; BPSK; pulse generator; passive mixer; driver amplifier; IR-UWB
DOI: 10.1088/1674-4926/31/9/095005 **EEACC:** 1250; 2570D

1. Introduction

Ultra-wide band (UWB) has been shown to be promising technology for short range high data rate wireless communication. It has received significant interest from researchers and industries since the Federal Communications Commission (FCC) allocated 7.5 GHz of the spectrum from 3.1 to 10.6 GHz for unlicensed use in 2002[1]. The IEEE 802.15.3a Task Group has been withdrawn because an agreement could not be reached on the high data rate UWB standards[2]. The WiMedia Alliance will also shut down after handing over all specification development of its version of UWB to the Bluetooth Special Interest Group, the Wireless USB Promoter Group and the USB Implementers Forum. It is extremely possible that UWB will be merged into Bluetooth 3.0 and/or Wireless USB[3].

Though FCC opened the frequency range of 3.1–10.6 GHz, most researchers concentrate on the low band of 3.1–5 GHz because it is relatively easy to realize with a moderate CMOS process. In general, the reported transmitters can be divided into three categories, multi-carriers, single-carrier and carrier-free. The multi-band OFDM (MB-OFDM) UWB systems use multi-carriers[4, 5]. This offers flexibility in terms of meeting different spectral requirements since the power levels of different bands can be adjusted independently. However, the use of multi-carriers and sub-band selection results in complex system design[6].

Carrier-free and single-carrier transmitters are used in impulse radio UWB (IR-UWB) systems. The carrier-free systems directly transmit extremely short pulses on the order of a nanosecond or less, which occupy a bandwidth up to several GHz[6–8]. The Gaussian monocycle and its derivatives are often utilized as the transmitted pulse since they provide smaller side lobes and a sharper roll-off in the frequency domain as compared to other pulse types. However, one needs to use at least the fifth derivative of Gaussian pulse to comply with the FCC spectral mask for indoor UWB applications[9]. Therefore, a low order Gaussian pulse is firstly produced and then a filter (differentiator) is commonly employed to shape the pulse in these transmitters. According to Ref. [10], a small variation on the σ (standard deviation) value causes the center frequency to drift significantly and higher frequencies are more affected than lower frequencies. It is not an easy task to control the spectral mask of the pulse under various temperatures and processes.

In single-carrier UWB systems, there are generally two methods to generate FCC compliant pulses, the switch-based method and the up-conversion method. In the former, a narrow-pulse is produced first and then the pulse is used to control the switching on and off of the oscillator[11, 12]. It is power-efficient because the oscillator is not working and consuming power most of the time due to the low duty cycle of the pulse. Nevertheless, it is only suitable for on-off keying (OOK) or pulse-position modulation (PPM) and energy-detected receivers. In the latter method, the baseband pulse with a low-pass spectrum is up-converted in frequency using the LO by a mixer. The center frequency and the bandwidth can be regulated flexibly by the LO and the baseband pulse separately. For this reason, it is convenient to make the power spectrum density (PSD) of the pulse comply with the FCC mask.

In this paper, a BPSK transmitter based on up-conversion for IR-UWB is proposed. The quasi-Gaussian pulse is firstly produced and then shifted to high frequency by a high linearity passive mixer to comply with the FCC mask. Unlike the traditional BPSK modulation scheme, the LO instead of the pulse is modulated by the baseband data.

2. Transmitter design

2.1. Modulation scheme and transmitter topology

The performance of UWB systems is strongly dependent on the multi access and modulation scheme. Typically, three modulation schemes are employed most in IR-UWB systems. They are OOK, PPM and BPSK. In this transmitter, the BPSK scheme is utilized because of its better performance in multi-

* Project supported by the National High Technology Research and Development Program of China (No. 2007AA01Z2b2).
† Corresponding author. Email: luhuang@ustc.edu.cn
Received 24 February 2010, revised manuscript received 28 March 2010

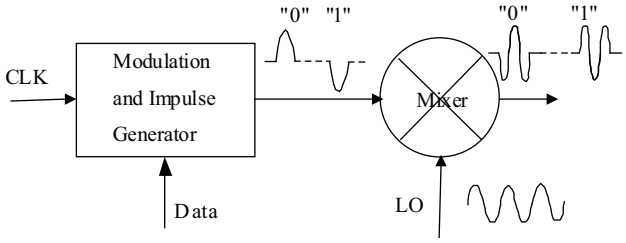

Fig. 1. Traditional BPSK transmitter.

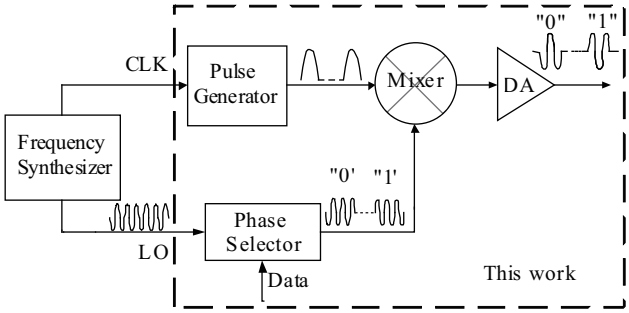

Fig. 2. Improved transmitter.

path environments. Firstly, the increase of the power spectral density levels in BPSK due to the multi-path is less than PPM or OOK. Secondly, the bit error rate (BER) of a system with the same E_b/N_0 using BPSK is lower than others as proposed in Ref. [13].

The signal based on BPSK can be written as

$$s(t) = \sum_{k=-\infty}^{\infty} a_k p(t - kT) \cos(2\pi f_0 t), \tag{1}$$

where T is the pulse repetition period, the sequence $\{a_k\}$ represents the binary information symbol, $a_k \in \{1, -1\}$, f_0 is the carrier frequency, and $p(t)$ is the baseband pulse. The traditional BPSK transmitter structure[14, 15, 18] according to Eq. (1) is illustrated in Fig. 1.

In the traditional transmitter the pulse is modulated by the data before up-conversion by the mixer. However, there is a disadvantage in this topology. Symmetry in phase and amplitude of the pulse is strictly required in the coherent receivers because the BER is highly sensitive to symmetry. Nevertheless, it is difficult to generate a differential, extremely short pulse which is a wideband signal.

$$s(t) = \sum_{k=-\infty}^{\infty} p(t - kT) [a_k \cos(2\pi f_0 t)]. \tag{2}$$

Noting that Equation (1) can be rewritten as Eq. (2), we propose the improved transmitter shown in Fig. 2.

In the proposed transmitter, the clock signal drives the pulse generator (PG) to produce an extremely short pulse with fixed period. Information is modulated by selecting the phase of the LO with the phase selector (PS). When the data is "0", it selects the LO phase "0". Otherwise, it selects the phase "π". Consequently, the external frequency synthesizer should provide a differential LO signal. This is much easier than generating a differential pulse because the LO signal is a single

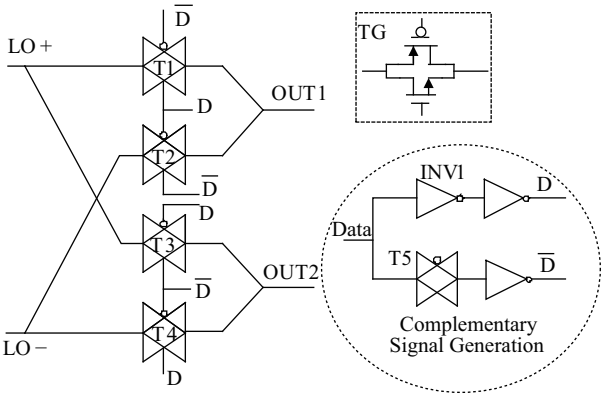

Fig. 3. Phase selector.

frequency one. This transmitter separates the pulse generation and modulation and avoids differential pulse generation. The driver amplifier (DA) is employed to amplify the up-converted pulse and drive the external antenna. The circuits in the dashed area will be introduced in the following section.

2.2. PS

The PS is illustrated in Fig. 3. It consists of 4 transmission gates (TGs). A TG is utilized as the switch instead of single nMOS or pMOS because the TG has a smaller on resistance and can reduce the influence of channel charge injection. Complementary signals are needed for the on-off of the transmission gate. The signals are generated by the right circuit in Fig. 3. T5 is employed for delay compensation introduced by INV1[16]. LO+ and LO– stem from the differential output of the external frequency synthesizer. The transmitted baseband data is applied to the input of the complementary signal generation circuit. When D is "1", T1 and T4 turn on and T2 and T3 turn off, thus OUT1 selects LO+ and OUT2 selects LO–. In contrast, OUT1 equals LO– and OUT1 equals LO+ when D is "0".

2.3. Pulse generation

As mentioned above, the Gaussian pulse has smaller side lobes and a sharper roll-off in the frequency domain. A zero-order Gaussian pulse can be time-defined by

$$p(t) = \frac{1}{\sqrt{2\pi}\sigma} \exp\left(-\frac{t^2}{2\sigma^2}\right), \tag{3}$$

where σ is the standard deviation of the Gaussian. The up-converted pulse can be written as

$$x(t) = \frac{1}{\sqrt{2\pi}\sigma} \exp\left(-\frac{t^2}{2\sigma^2}\right) \cos(2\pi f_0 t). \tag{4}$$

The Fourier transform of Eq. (4) is

$$G(f) = \frac{1}{2} \exp\left\{-\frac{[2\pi\sigma(f + f_0)]^2}{2}\right\} + \frac{1}{2} \exp\left\{-\frac{[2\pi\sigma(f - f_0)]^2}{2}\right\}, \tag{5}$$

and then the PSD of the transmitted signal equation (2) is[17]

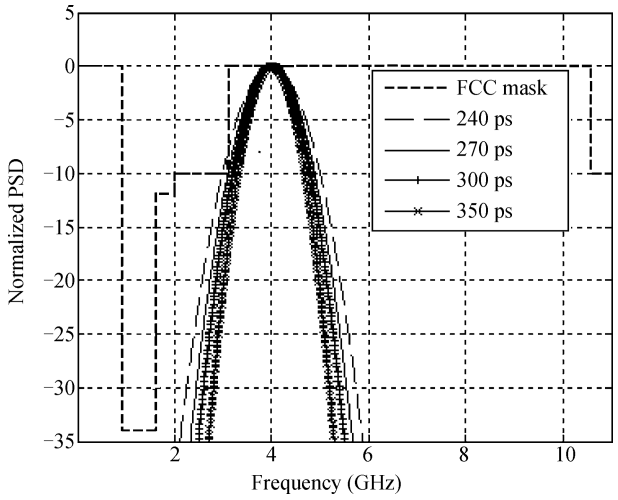

Fig. 4. Normalized PSD with different σ for indoor UWB.

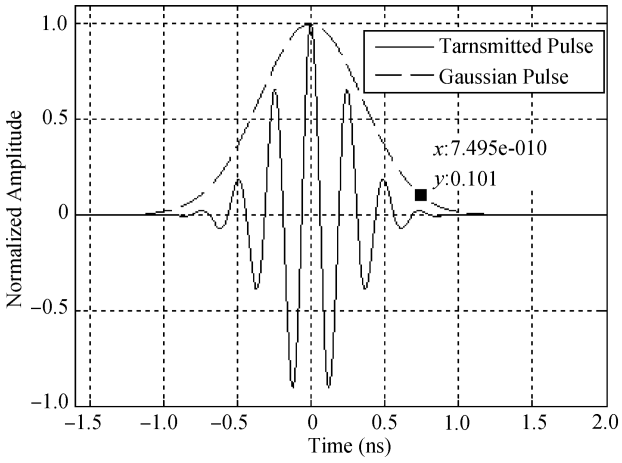

Fig. 5. Pulse waveform with $\sigma = 270$ ps.

$$S(f) = \frac{\sigma_{\mathrm{a}}^2}{T}|G(f)|^2 + \frac{\mu_{\mathrm{a}}^2}{T^2}\sum_{-\infty}^{\infty}\left|G\left(\frac{k}{T}\right)\right|^2 \delta\left(f - \frac{k}{T}\right), \quad (6)$$

where σ_{a}^2 and μ_{a} are the variance and mean of the symbol sequence $\{a_k\}$ and $\delta(\bullet)$ is the Dirac delta function. The second term in Eq. (6) means the discrete spectral lines which will vanish if the information symbols have zero mean. Assuming $\sigma_{\mathrm{a}}^2 = 1$ and $\mu_{\mathrm{a}} = 0$, we rewrite Eq. (6) as

$$S(f) = \frac{1}{T}|G(f)|^2. \quad (7)$$

According to Eqs. (5) and (7), the spectral mask can be easily adjusted by changing the central frequency f_0 and the standard deviation σ. The latter determines the duration of the pulse. For the low band application, we make $f_0 = 4$ GHz. Meanwhile, the maximum of PSD is proportional to the amplitude and repetition frequency of the pulse. The normalized PSD with different σ is shown in Fig. 4. We can see that the pulse with $\sigma = 270$ ps is the best option as it occupies the largest bandwidth while meeting the FCC spectrum regulation. The Gaussian pulse and up-converted pulse with $\sigma = 270$ ps

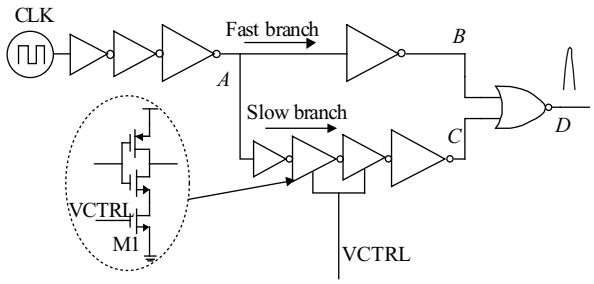

Fig. 6. Proposed PG.

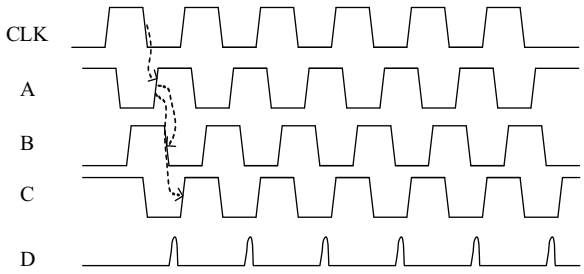

Fig. 7. Timing diagram of the PG.

are illustrated in Fig. 5. The 10%–10% width of the Gaussian pulse is about 1.2 ns.

The schematic of the pulse generator (PG) is illustrated in Fig. 6. After being driven by the inverters, the clock signal is split into two delay branches, the fast branch and the slow branch. In the fast branch, the clock signal is delayed by one inverter, whereas it is delayed by four inverters in the slow branch. The delay time of the slow branch is controlled by VCTRL because the on resistance of M1 changes with the change of VCTRL. The NOR combines the falling edge of the signal from node B and the rising edge of the signal from node C to form a quasi-Gaussian pulse. The pulse width is determined by the delay between the falling edge and the rising edge. Thus, the duration is adjustable. A detailed timing diagram of the PG is given in Fig. 7.

2.4. Mixer and DA

The Gilbert mixer is used widely in transceivers because it provides conversion gain that can reduce the noise contribution of the following blocks for the system. Also, it has low LO leakage and low even order distortion products at the output. However, the Gilbert mixer has poor linearity due to the voltage-to-current conversion by the transconductor stage and the stack topology. In addition, it has large power dissipation[18]. In the proposed transmitter, the amplitude of the pulse from the PG is large. Hence, high linearity is required for the up-conversion mixer. The Gilbert mixer is not suitable for the transmitter. The FET resistive ring mixer is an attractive candidate. Though it has conversion loss, it denotes excellent linearity and does not require DC bias current. The resistive FET mixer with LO buffer and DA are depicted in Fig. 8.

As shown in Fig. 8, the FET resistive ring mixer consists of four nFETs. The modulated LO from PS is first amplified by the LO buffer and then applied to the gates of the nFETs

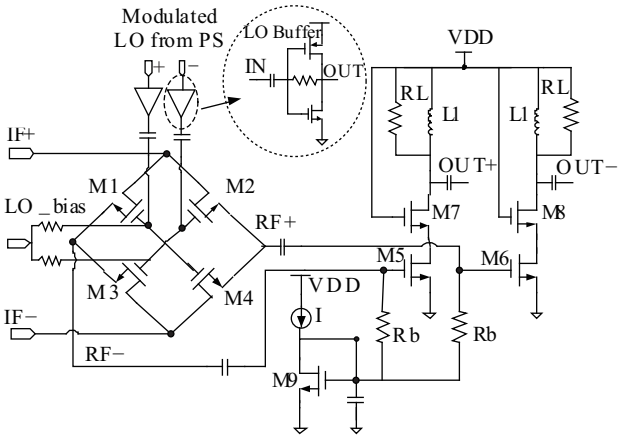

Fig. 8. Mixer and DA.

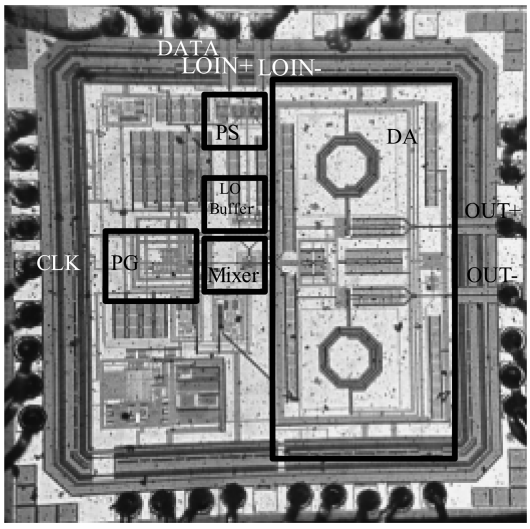

Fig. 9. Chip micrograph of the transmitter.

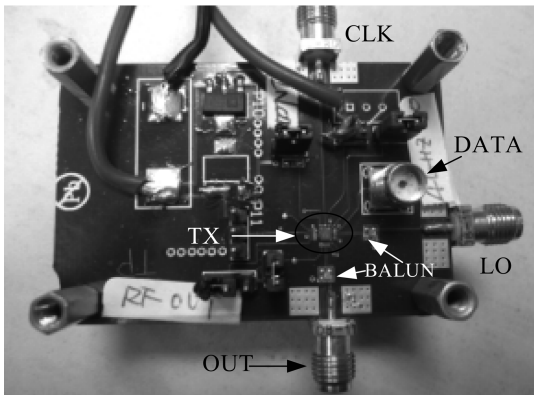

Fig. 10. Test board of the transmitter.

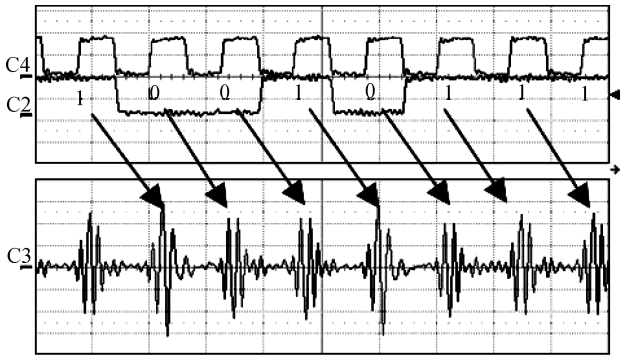

Fig. 11. Measured transmitter output.

which are biased at the threshold voltage. The self-bias inverter is employed as the LO buffer to eliminate the bias circuit of the buffer. The core transistors M1–M4 act as switches. On the positive half cycle of LO, M1 and M4 switch on, M2 and M3 switch off, and vice versa. The mixer has very low levels of intermodulation distortion because of the good linearity of the channel resistance when the transistor is on and operating in the deep triode region. The fully differential structure of the mixer provides virtual grounds at each port. Therefore port-to-port isolation is inherent in the mixer[19].

For our application, the pulse from PG is single-ended. For simplicity, it is applied to the port IF+, while keeping IF– connected to ground. The pulse is alternatively passed through to the RF port, and hence shifted to the high frequency centered LO frequency. The conversion loss, NF and linearity of the mixer are dependent on the sizes of the four transistors and LO amplitude[19]. Thus, a trade-off must be made on the sizes. Here, 80 μm/0.18 μm of W/L is used for high linearity, moderate conversion loss and NF. The driver amplifier employs cascode topology. The inductor L_1 resonates with the capacitor at 4 GHz and the resistance R_1 is used to lower the output resistance of the amplifier and match 100 Ω differential impedance. The gain of DA can be adjusted by varying the bias current I.

3. Measured results

The proposed transmitter was implemented in 0.18 μm 1P6M RF CMOS technology. Figure 9 depicts the chip micrograph. The chip area including ESD-protected pads is 1.4×1.4 mm^2.

Chip on board (COB) technology is utilized for the measurement. The test board is shown in Fig. 10. The LO signal is converted to a differential by an external balun BD3150N50100A00 with a typical insert loss of 0.6 dB, and the differential output of the transmitter is converted to a single-ended signal by the same balun. The pulse output waveform is measured by the oscilloscope LeCroy WavePro 760 Zi. The data and clock are given by an Agilent 81134A dual-channel pulse pattern generator. In Fig. 11, C4 and C2 represent the inverted clock and inverted data separately, and C3 represents the output. A pseudo-random binary sequence (PRBS) is applied to the data input terminal of the transmitter. As presented in Fig. 11, a maximum pulse repetition frequency (PRF) of 400 MHz is achieved. The pulse amplitude can be adjusted by the LO amplitude and the bias current of DA. The maximum peak-to-peak amplitude reaches 600 mV. Under the circumstances, the transmitter consumes 20.3 mA with a supply voltage of 1.8 V. Hence, the energy efficiency is 91.4 pJ/pulse.

Limited by the performance of the spectrum analyzer HP8562A, the PSD of the transmitted pulse is measured with two frequency bands. Figures 12(a) and 12(b) represent the band 150 MHz–2.9 GHz and the band 2.75–11 GHz respec-

Table 1. Transmitter performance comparison.

Reference	This work	Ref. [6]*	Ref. [7]**	Ref. [10]*	Ref. [14]**	Ref. [18]*
Frequency (GHz)	3–5	3.1–10.6	3–5	3–5	3–5	3–5
Modulation scheme	BPSK	BPSK + PPM	PPM	PPM	BPSK	BPSK/OOK
Max PRF(MHz)	400	1800	400	40	1000	62
Max peak-to-peak amplitude/power	600 mV	220 mV	–9 dBm	200 mV	–9 dBm	250 mV
Energy efficiency (pJ/pulse)	91.4	126.1	190	50	105	299
Die area (mm^2)	1.96	2.83	4.42	NA	9.3	1.89
Technology (μm)	0.18	0.09	0.18	0.18	0.18	0.18

*TX only; **TX + RX.

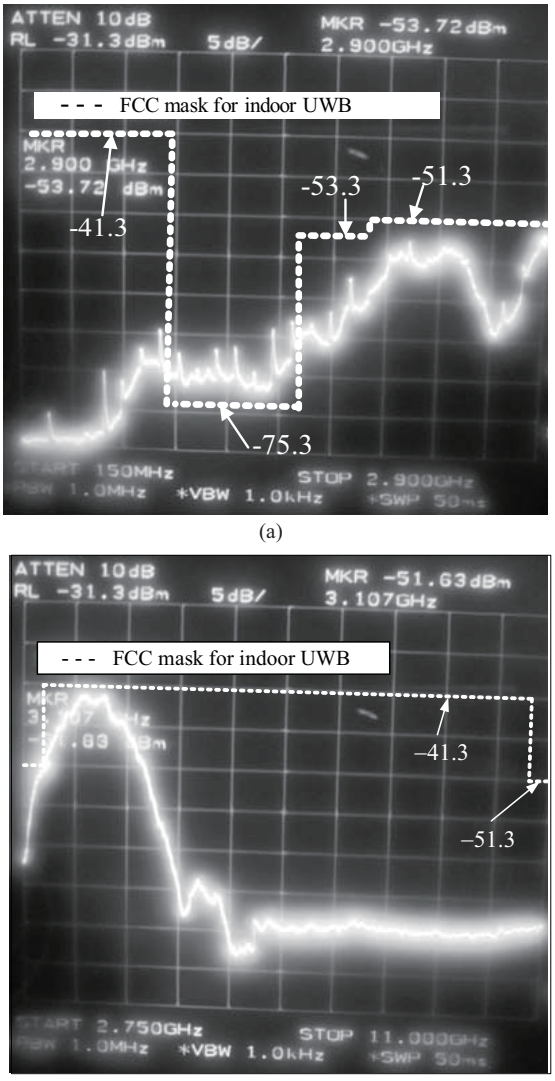

Fig. 12. Measured PSD with FCC mask for indoor UWB. (a) PSD for 150 MHz–2.9 GHz. (b) PSD for 2.75–11 GHz.

tively. It can be seen that the spectrum is well below the FCC spectral mask for indoor UWB communication systems besides the band 960 MHz–1.61 GHz. The PSD of the band 960 MHz–1.61 GHz is about 3 dBm/MHz higher than the FCC mask. This is because the produced baseband pulse is a non-ideal Gaussian pulse and thus has biggish side lobes in this band. Nevertheless, it can be facilely suppressed to meet the FCC mask by the UWB antenna with a band-pass characteristic.

4. Conclusion

A 3–5 GHz BPSK transmitter based on up-conversion for IR-UWB is presented in this paper. A quasi-Gaussian pulse is first produced and is then up-converted to high frequency with a high linearity passive mixer. Unlike the traditional BPSK modulation transmitter, the LO instead of the pulse is modulated by the baseband data. Designed and fabricated with 0.18 μm CMOS technology, the transmitter achieves a high data rate up to 400 Mbps. The amplitude of the pulse can be adjusted by the amplitude of the LO and the bias current of the DA. The maximum peak-to-peak amplitude of the pulse is 600 mV. The performance of the proposed transmitter compared with other recently reported transmitters is summarized in Table 1. It shows high energy efficiency because none of the modules, except the DA, consume any static power. The transmitter can be used for short-range high data rate or middle-range low data rate communication.

References

[1] Revision of Part 15 of the commission's rules regarding ultra-wide-band transmission systems: first report and order. Federal Communications Commission, Washington, DC, 2002, ET-docket 98-153, FCC 02-48
[2] IEEE 802.15 Task Group 3a. Online Available: http://www.ieee802.org/15/pub/TG3a.html
[3] Online Available: http://www.wimedia.org
[4] Razavi B, Aytur T, Lam C, et al. A UWB CMOS transceiver. IEEE J Solid-State Circuits, 2005, 40: 2555
[5] Sandner C, Derksen S, Draxelmayr D, et al. A WiMedia/MBOA-compliant CMOS RF transceiver for UWB. IEEE J Solid-State Circuits, 2006, 41: 2787
[6] Demirkan M, Spencer R R. A pulse-based ultra-wideband transmitter in 90-nm CMOS for WPANs. IEEE J Solid-State Circuits, 2008, 43: 2820
[7] Zheng Y, Tong Y, Ang C W, et al. A CMOS carrier-less UWB transceiver for WPAN applications. IEEE International Solid-State Circuits Conference, 2006: 378
[8] Wang Y, Kilambi S M, Gaudet V, et al. A low power CMOS transmitter design for IR-UWB communication systems. IEEE International Conference on Ultra-Wideband, 2007: 823
[9] Sheng H S, Orlik P, Haimovich A M, et al. On the spectral and power requirements for ultra-wideband transmission. IEEE International Conference on Communications, 2003, 1: 738
[10] Ryckaert J, Desset C, Fort A, et al. Ultra-wide-band transmitter for low-power wireless body area networks: design and evaluation.

IEEE Trans Circuits Syst, 2005, 52: 2515
[11] Xu R, Jin Y, Nguyen C. Power-efficient switching-based CMOS UWB transmitters for UWB communications and Radar systems. IEEE Trans Microw Theory Tech, 2006: 3271
[12] Sim S, Kim D W, Hong S. A CMOS UWB pulse generator for 6–10 GHz applications. IEEE Microw Wireless Compon Lett, 2009: 83
[13] Saad P, Botteron C, Merz R, et al. Performance comparison of UWB impulse-based multiple access schemes in indoor multipath channels. Proc IEEE WPNC, 2008: 89
[14] Zheng Y J, Wong K W, Asaru M A, et al. A 0.18 μm CMOS dual-band UWB transceiver. IEEE International Solid-State Circuits Conference, 2007
[15] Iida S, Tanaka K, Suzuki H, et al. A 3.1 to 5 GHz CMOS DSSS UWB transceiver for WPANs. IEEE International Solid-State Circuits Conference, 2005
[16] Razavi B. Design of analog CMOS integrated circuits. Beijing: The McGraw-Hill Education (Asia) Co & Tsinghua University Press, 2006: 334
[17] Proakis J G. Digital communications. New York: McGraw-Hill, 1995: 207
[18] Leow S W, Wong K W, Diao S X, et al. A 0.18 μm CMOS UWB transmitter with reconfigurable pulse width. Asia Pacific Microwave Conference, 2009: 253
[19] Son S W. High dynamic range CMOS mixer design. PhD Thesis, UC Berkeley, 2002